

See discussions, stats, and author profiles for this publication at: <https://www.researchgate.net/publication/231639887>

# Quantum-Chemical Investigation of the Conformational Dynamics of Mono-meso-phenyl-Substituted Octaalkylporphyrins in the Triplet Excited State

ARTICLE in THE JOURNAL OF PHYSICAL CHEMISTRY A · JUNE 2004

Impact Factor: 2.69 · DOI: 10.1021/jp048930i

---

CITATIONS

11

---

READS

10

4 AUTHORS, INCLUDING:



É. I. Zenkevich

Belarusian National Technical University

135 PUBLICATIONS 981 CITATIONS

SEE PROFILE



E. I. Sagun

National Academy of Sciences of Belarus

99 PUBLICATIONS 438 CITATIONS

SEE PROFILE

# Quantum-Chemical Investigation of the Conformational Dynamics of Mono-*meso*-phenyl-Substituted Octaalkylporphyrins in the Triplet Excited State

Igor V. Avilov,<sup>\*,†,‡</sup> Eduard I. Zenkevich,<sup>‡</sup> Evgeny I. Sagun,<sup>‡</sup> and Igor V. Filatov<sup>‡</sup>

Laboratory for Chemistry of Novel Materials, University of Mons-Hainaut, Materia Nova, Place du Parc 20, B-7000 Mons, Belgium, and Institute of Molecular and Atomic Physics, National Academy of Sciences of Belarus, F. Skaryna Ave. 70, 220072 Minsk, Belarus

Received: March 10, 2004; In Final Form: April 29, 2004

The detailed theoretical analysis (semiempirical PM3, DFT, and TD-DFT calculations) of the nature of nonplanar conformations of sterically encumbered mono-*meso*-phenyl-substituted octaalkylporphyrins in the excited triplet state has been carried out. It was found that the OEP-*meso*Ph molecule in the triplet excited state may occur in the highly nonplanar conformation characterized by the out-of-plane displacement of the single C<sub>m1</sub>–C<sub>1</sub> bond and the increased overlap of the porphyrin and the *meso*-phenyl ring. For the sterically strained porphyrins, the transition into this nonplanar conformation is accompanied by the essential decrease of the vertical triplet–singlet energy gap  $\Delta E_V(T_1-S_0)$  down to 0.45 eV, in contrast to  $\Delta E_V(T_1-S_0) \sim 1.33$  eV for the planar conformation. This leads to the experimentally detected drastic reduction of the triplet state decays for the sterically strained OEP-*meso*Ph type molecules. The calculated  $T_1 \rightarrow T_n$  transient absorption spectra for planar and nonplanar conformations have been compared with the corresponding experimental data obtained for the investigated compounds. A remarkable accord between experimental results and theoretical calculations on  $T_1 \rightarrow T_n$  absorption spectra in the red and near-IR region provides additional support for the conformational reorganization leading to the formation of the highly nonplanar distortion of OEP-*meso*Ph molecule in the triplet excited state.

## I. Introduction

At present, available literature crystallographic data indicate that tetrapyrrole compounds found in natural systems (photosynthetic light-harvesting complexes<sup>1,2</sup> and reaction centers,<sup>3</sup> hemoproteins,<sup>4,5</sup> vitamin B<sub>12</sub><sup>6</sup>) are characterized by different nonplanar conformations caused by the interactions with the protein environment. In addition, the nonplanarity of tetrapyrrole macrocycles due to steric hindrance effects takes place in artificial supramolecular systems modeling the energy and electron-transfer processes in vivo.<sup>7,9</sup> Crystallographic<sup>10–12</sup> and spectral-luminescence methods<sup>13–15</sup> revealed the deviation from planarity for a number of individual tetrapyrrole compounds both in crystalline form and liquid solutions.<sup>10</sup> These results have led to the concept of the conformational design of porphyrins, when the nonplanarity of the macrocycle and the form of distortion are directed by the steric interactions of the peripheral bulky substituents at  $\beta$ - and *meso*-positions of the tetrapyrrole macrocycle.<sup>16–18</sup>

Typical examples of sterically strained  $\pi$ -conjugated tetrapyrroles are the so-called “hybrid porphyrins” based on octaalkylporphyrins (octaethyl, OEP, or octamethylporphyrins, OMP) and tetraphenylporphyrins (TPP) and characterized by strong spectral, photophysical and electrochemical manifestations of the nonplanar distortions of the porphyrin macrocycle. With respect to normal planar porphyrins, these compounds exhibit large Stokes and bathochromic shifts of the absorption

and fluorescence bands as well as drastic shortening of the excited singlet and triplet states decays.<sup>16–21</sup>

As for tetra-*meso*-substituted octaalkylporphyrins, the strengthening of the nonradiative deactivation of S<sub>1</sub> and T<sub>1</sub> states has been associated mainly with the macrocycle nonplanarity, present already in the ground S<sub>0</sub> state. Consequently, there was no reason to study mono- and 5,15-aryl-substituted OEP or OMP molecules, planar in the ground state, from this point of view. It was assumed that for the latter compounds the energetics and spectral luminescent properties have to be close to those for planar porphyrins. Nevertheless, we have shown experimentally for the first time that the excited T<sub>1</sub> states of OEP or OMP molecules are very sensitive to mono- and 5,15-aryl-substitution, even in conditions where spectral kinetic parameters of S<sub>0</sub> and S<sub>1</sub> states remain unchanged. We have proven that at room temperature in degassed toluene solutions, mono- and 5,15-*meso*-phenyl substitution in OEP molecules (free bases and Zn complexes) leads to the drastic shortening of T<sub>1</sub> state decays (by  $\sim 300$ –1000 times) without any influence on the spectral kinetic parameters of S<sub>0</sub> and S<sub>1</sub> states.<sup>22</sup> This quenching was attributed to torsion vibrations (librations) of the phenyl ring around a single C<sub>m1</sub>–C<sub>1</sub> bond in sterically encumbered OEPs (see Figure 1) leading to nonplanar dynamic distorted conformations realized in the excited T<sub>1</sub> state only.<sup>22–24</sup> Two triplet conformers having “mother–daughter” relationship and vastly different photophysical properties for 5,15-diaryloctaalkylporphyrins in liquid solutions at 295 K have been found later by other groups.<sup>25,26</sup> We have also observed that the rate constants of nonexponential decays of T<sub>1</sub> states in *meso*-phenyl-substituted OMP molecules differ significantly from those found for *meso*-phenyl-substituted OEPs.<sup>27</sup> This difference is connected with

\* Corresponding author: Present address: University of Mons-Hainaut, Belgium. Fax: +32 65 373861; E-mail: avilovi@averell.umh.ac.be. Permanent address: National Academy of Sciences of Belarus.

<sup>†</sup> University of Mons-Hainaut, Materia Nova.

<sup>‡</sup> National Academy of Sciences of Belarus.

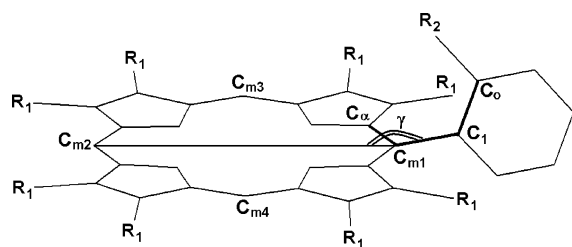


**Figure 1.** Schematic representation of the chemical structure for the compounds under study. OEP-*meso*Ph:  $R_1 = C_2H_5$ ,  $R_2 = H$ . OEP-*meso*Ph(*o*-CH<sub>3</sub>):  $R_1 = C_2H_5$ ,  $R_2 = CH_3$ . OMP-*meso*Ph:  $R_1 = CH_3$ ,  $R_2 = H$ ; P-*meso*Ph:  $R_1 = R_2 = H$ . In calculations, alkyl groups on the pyrroles distant from the phenyl ring were substituted on hydrogen atoms. We believe that the absence of these alkyl groups should result in minor influence on the photophysical properties of the systems under study. The dihedral angle  $\beta$  (marked with bold lines) is formed by the atoms  $C_\alpha-C_{m1}-C_1-C_0$ . The angle  $\gamma$  is formed by  $C_{m2}-C_{m1}$  and  $C_{m1}-C_1$  axes.

different conditions for the steric interactions of the phenyl ring with neighboring  $\beta$ -CH<sub>3</sub> and  $\beta$ -C<sub>2</sub>H<sub>5</sub> substituents, correspondingly.

In this respect it should be noted that the majority of the information on the nature and type of the macrocycle distortion (usually obtained by the X-ray and NMR spectroscopy) is related to the ground (not excited) state of porphyrins. Meanwhile, the available data concerning the conformational distortions for sterically strained porphyrins in the excited states (in the triplet states, particularly) are scarce. For example, using time-resolved EPR data it was elucidated that in a liquid crystal matrix the octaethyltetraphenylporphyrin molecule (H<sub>2</sub>-OETPP) may be characterized by simultaneous presence of two types of triplets.<sup>28</sup> In addition, time-resolved experiments (transient triplet-triplet absorption spectroscopy) in liquid solutions at 295 K have shown the existence of conformational realignments in the excited triplet states for 5,15-diaryloctaalkylporphyrins (Zn complexes and free bases<sup>25,26</sup>) as well as for 5,10- and 5,10,15-phenyl-substituted OMP molecules.<sup>27</sup>

It should be mentioned also that at 295 K in liquid toluene the transient  $T_1 \rightarrow T_n$  absorption spectra (in the region of 700–1600 nm) for sterically strained porphyrins (*meso*-phenyl-substituted OEP and PdOEP) are distinguished from those measured for usual planar tetrapyrroles.<sup>22,29</sup> The appearance of new bands in the red and IR regions of  $T_1 \rightarrow T_n$  absorption spectra of sterically strained porphyrins with respect to the spectra of normal planar tetrapyrroles may be connected with the nonplanar distortion of the porphyrin macrocycle in the former molecules.

In this paper, we carry out the detailed theoretical analysis of the character of nonplanar conformations for sterically encumbered porphyrins in the excited triplet state. We present also calculated  $T_1 \rightarrow T_n$  transient absorption spectra for planar and nonplanar conformations of the investigated compounds. The calculated spectroscopic and photophysical characteristics of triplet states are compared with the corresponding experimental data obtained in our group earlier.

## II. Computational Details

Molecular dynamics simulations were performed for OEP-*meso*Ph and OMP-*meso*Ph molecules by the semiempirical PM3 method<sup>30,31</sup> realized in the quantum-chemical package HyperChem (release 4, HyperCube Inc.), using the unrestricted Hartree–Fock (UHF) self-consistent field<sup>32</sup> formalism. Parameters of the simulations were chosen as follows: time step  $\Delta t = 0.001$  ps, bath relaxation time BRT = 0.1 ps. The simulations were carried out in two steps: at the first step the system was

heated from 0 to 300 K within 50 ps, at the second step the simulations were done during the next 50 ps at constant temperature of 300 K. PM3 (UHF) optimized structures were used as the starting geometry.

DFT calculations were performed using Becke's three-parameter hybrid functional B3LYP.<sup>33,34</sup> Unrestricted B3LYP (UB3LYP) formalism was used for the triplet state calculations, while the ground-state calculations were done using the restricted SCF version (B3LYP).<sup>35</sup> The  $\langle S^2 \rangle$  values for all triplets are below 2.07. The calculations of transient  $T_1 \rightarrow T_n$  absorption spectra were carried out by time-dependent density functional response theory (TD-DFT).<sup>36,37</sup> The structures of planar, saddle-shaped, and nonplanar conformations of OEP-*meso*Ph, as well as planar and nonplanar conformations of OMP-*meso*Ph, and nonplanar conformation of OEP-*meso*Ph(*o*-CH<sub>3</sub>) were verified to be minima by calculating the matrix of the second derivatives of energy (Hessian). All calculations were performed using double- $\zeta$  basis sets 6-31G (for geometry optimization) and 6-31G(d) (for calculations of  $T_1 \rightarrow T_n$  spectra)<sup>38,39</sup> implemented in the Gaussian 98 (revision A. 11) suit of programs.<sup>40</sup>

## III. Results and Discussion

**A. Transient Triplet–Triplet Absorption Spectra.** Experimental transient  $T_1 \rightarrow T_n$  absorption spectra obtained for sterically hindered and planar molecules of OEP-type in toluene at 295 K<sup>22</sup> show the following principal differences (see Figure 2). As it is seen in Figure 2A, the  $T_1 \rightarrow T_n$  absorption spectrum in the near-IR region down to 1660 nm for sterically hindered OEP-*meso*Ph molecule is characterized by a new band with the maximum at 1000 nm and a large half-width. In contrast, in the  $T_1 \rightarrow T_n$  absorption spectrum for a planar OEP molecule this band is absent. In the latter case the transient spectrum is characterized by the monotonic decrease of intensity in the near-IR region down to 1660 nm (see Figure 2B). According to ref 22, the presence of this long-wavelength band has to be related with the effect of the dynamic nonplanarity of the  $\pi$ -conjugated macrocycle. Really, this band is absent also in the transient  $T_1 \rightarrow T_n$  absorption spectrum for the planar OEP-*meso*Ph(*o*-CH<sub>3</sub>) molecule (see Figure 2C), in which the conformational reorganization is essentially limited due to the steric interactions of the neighboring bulky substituents, namely the CH<sub>3</sub> group in the ortho position of the *meso*-phenyl ring and the C<sub>2</sub>H<sub>5</sub> group in  $\beta$ -pyrrolic position of porphyrin macrocycle.<sup>22</sup>

**B. Analysis of the Model Proposed Earlier.** The geometry optimization in the triplet state of OEP-*meso*Ph molecule with different orientation of  $\beta$ -ethyl groups (as shown in Figure 3 A,B) was performed using the UB3LYP method. As one may see from Figure 3, the different orientation of the ethyl substituents leads alternatively to planar (A) and saddle-shaped (B) structures of the porphyrin macrocycle. In the case of saddle-shaped conformation, the dihedral angle  $\beta \sim 83^\circ$ , while for planar conformation the phenyl ring is perpendicular to the plane of the porphyrin macrocycle ( $\beta \sim 90^\circ$ ).

The authors of ref 26 proposed that namely the saddle-shaped distortion of the porphyrin macrocycle is responsible for the increased nonradiative decay of the triplet state of 5,15-phenyl OMP molecules. The reason of that was explained by the fact that the calculated vertical  $T_1-S_0$  energy gap  $\Delta E_V(T_1-S_0)$  is decreased by about 0.31 eV upon going from planar conformation to saddle-shaped conformation.<sup>26</sup> In contrast, our data for OEP-*meso*Ph molecule indicate that the difference of the energy gap  $\Delta E_V(T_1-S_0)$  for these two conformations is essentially smaller:  $\Delta E_V(T_1-S_0) = 1.34$  eV for the planar conformation and  $\Delta E_V(T_1-S_0) = 1.32$  eV for saddle-shaped one. In this

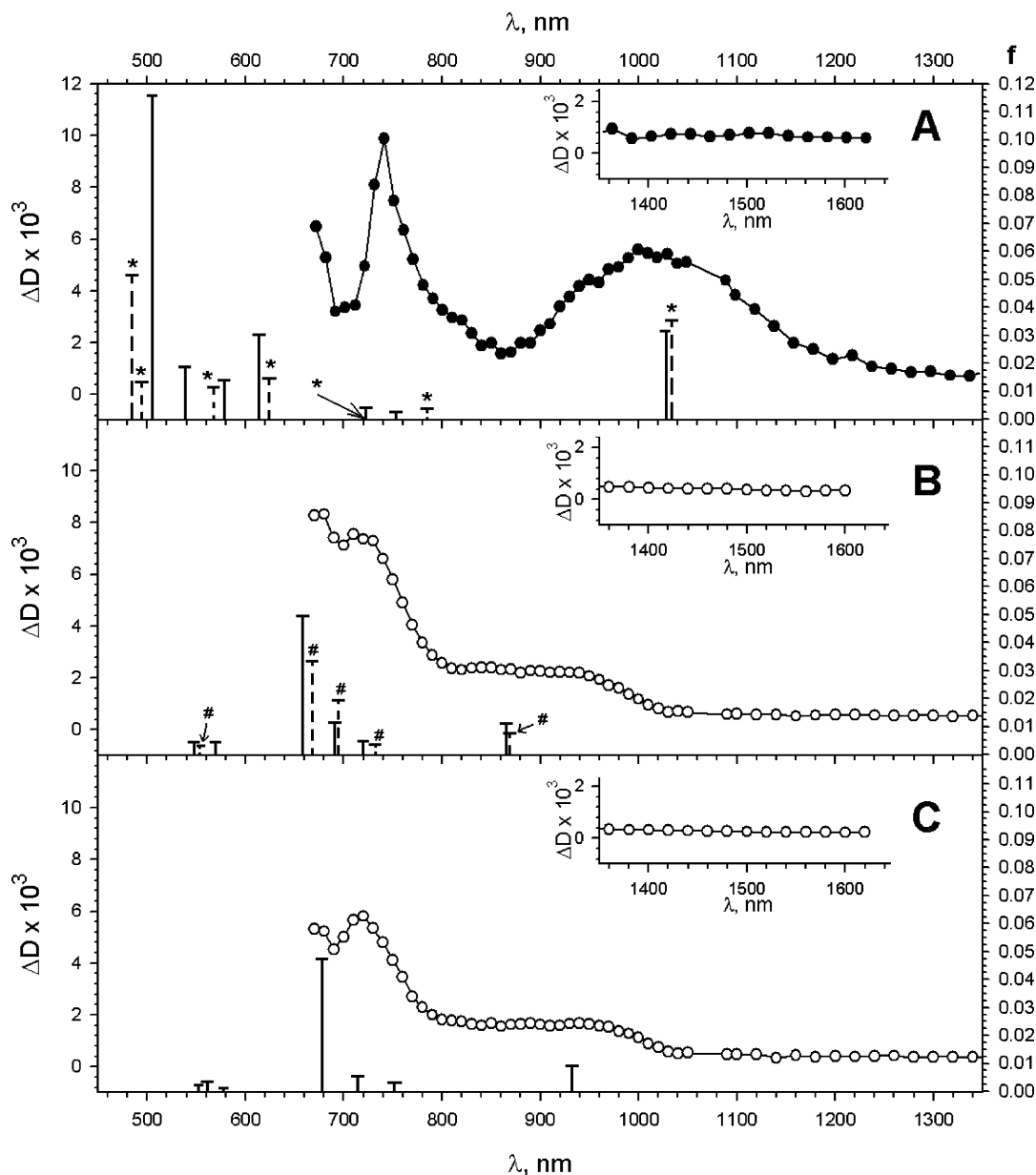


**Figure 2.** Experimental transient  $T_1 \rightarrow T_n$  absorption spectra for OEP-*meso*Ph (A), OEP (B), and OEP-*meso*Ph(*o*-CH<sub>3</sub>) (C) molecules. The insets show measured  $T_1 \rightarrow T_n$  absorption spectra in the near-IR region between 1350 and 1650 nm. Calculated electronic transitions and their relative intensities in  $T_1 \rightarrow T_n$  absorption spectra are shown by vertical rods for OEP-*meso*Ph molecule in the nonplanar (A, solid lines), planar (B, dashed lines marked by “#” sign), and saddle-shaped (C) conformations. For the nonplanar conformation of the OEP-*meso*Ph molecule, in which the phenyl ring was substituted by hydrogen (A, dashed lines marked by asterisks), one of the calculated transitions (marked by an arrow) practically coincides by its energy and intensity with the corresponding transition found for OEP-*meso*Ph in the nonplanar conformation; OEP (B, solid lines). Note that calculations were performed for structures without alkyl groups on the pyrroles distant from the phenyl ring.

respect, it should be particularly emphasized that the planar conformer in ref 26 was obtained artificially by restricting the phenyl ring to be orthogonal with respect to the porphyrin macrocycle plane.

The results of the calculated energies and oscillator strengths of the corresponding transitions in  $T_1 \rightarrow T_n$  absorption spectra for the optimized planar and saddle-shaped conformations for OEP-*meso*Ph are collected in Table 1 and are shown on Figure 2. The analysis of the results shows that these spectra are rather similar. Although the lowest energy transition in  $T_1 \rightarrow T_n$  absorption spectrum for the saddle-shaped conformation is red-shifted by 61 nm (750 cm<sup>-1</sup>), its intensity does not increase significantly in comparison with that for planar conformation. Correspondingly, the calculated  $T_1 \rightarrow T_n$  spectrum for saddle-shaped conformation of OEP-*meso*Ph molecule (see Figure 3B) does not correspond to the experimental spectrum characterized

by an intense red-shifted IR band with the maximum at 1000 nm. In this respect, it should be mentioned that our calculations show also that the addition of the methyl group into the ortho position of the phenyl ring of the OEP-*meso*Ph molecule in the saddle-shaped conformation does not force it to adopt a more planar conformation. At the same time, the triplet state lifetime in degassed toluene solution at 295 K increases to 1000  $\mu$ s for OEP-*meso*Ph(*o*-CH<sub>3</sub>) in comparison with 4  $\mu$ s for OEP-*meso*Ph.

Thus, it is obvious that the drastic shortening of the triplet state lifetime for OEP-*meso*Ph in liquid solutions ( $\tau_T^0 = 4.0 \mu$ s<sup>22</sup>) and the appearance of a new intense IR band in its  $T_1 \rightarrow T_n$  absorption spectrum should be connected with more serious conformational changes of the molecule in the triplet state. To characterize these conformational changes we carried out molecular dynamics simulations of the molecules in the excited  $T_1$  state.

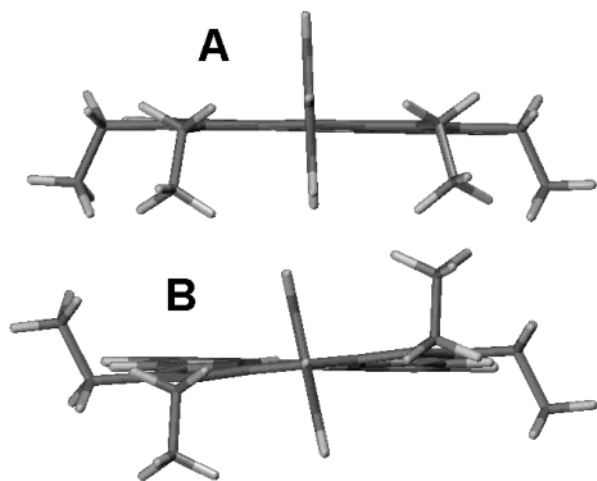


**Figure 3.** UB3LYP optimized planar (A) and saddle-shaped (B) conformations for OEP-*meso*Ph molecule in the  $T_1$  state. It is seen that the planar and saddle-shaped conformations are realized for different orientation of  $\beta$ -ethyl groups neighboring the *meso*-phenyl.

**C. Conformational Dynamics in the  $T_1$  State.** Molecular dynamics simulations in the triplet state showed that during the heating step OEP-*meso*Ph and OMP-*meso*Ph molecules adopted the highly nonplanar conformation (the image of the DFT-optimized nonplanar conformation is shown on Figure 4). This switch from planar to nonplanar conformation takes place in two steps. At the first step, the single  $C_{m1}-C_1$  bond goes out of the porphyrin plane, in the process the angle  $\gamma$  decreases down to  $\sim 130^\circ$ . Then the phenyl ring rotates about this single bond to the value of the dihedral angle  $\beta \sim 0^\circ$ . This transition to the nonplanar conformation occurs at the simulation temperature about 50–60 K.

We emphasize that the nonplanar conformations of this type had not been observed in the X-ray studies of the sterically strained porphyrins, which apparently points to the fact that these conformations occur only in the excited state.

To investigate in more detail the features of the triplet state potential energy surface (PES) of the compounds under study, we performed a series of restricted geometry optimizations with the fixed values of the dihedral angle  $\beta$ . Namely, in each calculation the angle  $\beta$  had a fixed value between 0 and  $90^\circ$ , at the same time all the other geometrical parameters of molecules were allowed to relax. The planar (corresponding to the largest value of the angle  $\beta$ ) and nonplanar (corresponding to the lowest value of the angle  $\beta$ ) conformations were optimized without any geometrical restrictions. In this manner we got a set of points on the triplet PES. Calculations of the ground-state total energy were carried out for the compounds under study (using the optimized structures for the triplet states) in order to estimate the vertical triplet–singlet energy gap  $\Delta E_V(T_1-S_0)$ .

The corresponding results are presented in Figure 5 for OEP-*meso*Ph (A), OEP-*meso*Ph(*o*-CH<sub>3</sub>) (B), OMP-*meso*Ph (C), and porphine-*meso*Ph molecule, P-*meso*Ph (D). It follows from the calculations that for all investigated compounds (with the exception of P-*meso*Ph) the single  $C_{m1}-C_1$  bond comes out from the porphyrin plane ( $\gamma \sim 120-130^\circ$ ) at the values of  $\beta \sim 60-70^\circ$ . Upon further decrease of the angle  $\beta$ , the angle  $\gamma$  does not change significantly, which is in good agreement with the results of the molecular dynamics simulation. For the cases presented in Figure 5, the barrier height of the transition into the nonplanar conformation and the energies of the planar and nonplanar conformations depend essentially on the nature of the  $\beta$  substituents (neighboring the phenyl ring) as well as on the presence of the bulky substituent in the ortho position of the

**TABLE 1: Calculated Wavelengths ( $\lambda$ , nm), Oscillator Strengths ( $f$ ), and CI Composition of Allowed Electronic Transitions in  $T_1 \rightarrow T_n$  Absorption Spectra of the OEP-*meso*Ph Molecule in the Planar, Saddle-Shaped, and Nonplanar Conformations**

state	$\lambda$ , nm	$f$	excitation <sup>a</sup>	weight, %
Planar				
1	872	0.0075	H-1 $\beta \rightarrow L \beta$	96
2	734	0.0034	H-2 $\beta \rightarrow L \beta$	81
			H $\alpha \rightarrow L+1 \alpha$	17
3	695	0.0193	H-3 $\beta \rightarrow L \beta$	47
			H $\alpha \rightarrow L+1 \alpha$	32
4	671	0.0338	H-3 $\beta \rightarrow L \beta$	49
			H $\alpha \rightarrow L+1 \alpha$	28
5	571	0.0009	H-3 $\beta \rightarrow L \beta$	49
			H $\alpha \rightarrow L+1 \alpha$	28
6	554	0.0035	H-1 $\alpha \rightarrow L \alpha$	53
			H $\beta \rightarrow L+2 \beta$	34
7	537	0.0005	H-8 $\beta \rightarrow L \beta$	76
			H-5 $\beta \rightarrow L \beta$	20
8	507	0.0003	H-10 $\beta \rightarrow L \beta$	94
Saddle-shaped				
1	933	0.0093	H-1 $\beta \rightarrow L \beta$	97
2	752	0.0028	H $\alpha \rightarrow L+1 \alpha$	11
			H-2 $\beta \rightarrow L \beta$	88
3	715	0.0051	H $\alpha \rightarrow L+1 \alpha$	12
			H-3 $\beta \rightarrow L \beta$	83
4	680	0.0475	H $\alpha \rightarrow L+1 \alpha$	55
			H-3 $\beta \rightarrow L \beta$	13
			H-2 $\beta \rightarrow L \beta$	9
			H $\beta \rightarrow L+2 \beta$	9
5	578	0.0014	H-4 $\beta \rightarrow L \beta$	91
6	561	0.0029	H-1 $\alpha \rightarrow L \alpha$	54
			H $\beta \rightarrow L+2 \beta$	40
7	553	0.0017	H-7 $\beta \rightarrow L \beta$	74
			H-5 $\beta \rightarrow L \beta$	12
nonplanar				
1	1027	0.0309	H $\alpha \rightarrow L \alpha$	65
			H $\beta \rightarrow L \beta$	25
2	754	0.0016	H-1 $\beta \rightarrow L \beta$	81
3	722	0.0038	H-2 $\beta \rightarrow L \beta$	44
			H $\alpha \rightarrow L+1 \alpha$	32
4	616	0.0303	H-2 $\beta \rightarrow L \beta$	40
			H $\beta \rightarrow L+2 \beta$	15
			H $\alpha \rightarrow L+1 \alpha$	15
			H-4 $\beta \rightarrow L \beta$	12
5	579	0.0142	H $\alpha \rightarrow L+1 \alpha$	31
			H-1 $\alpha \rightarrow L \alpha$	30
			H-2 $\alpha \rightarrow L \alpha$	26
6	539	0.0192	H $\beta \rightarrow L+1 \beta$	53
			H-2 $\alpha \rightarrow L \alpha$	23
7	505	0.1154	H-1 $\alpha \rightarrow L \alpha$	26
			H $\beta \rightarrow L+1 \beta$	23
			H-4 $\beta \rightarrow L \beta$	16
			H $\beta \rightarrow L+2 \beta$	12

<sup>a</sup> In the CI composition, H stands for HOMOs and L stands for LUMOs.

*meso*-phenyl. Of fundamental importance is the fact that upon transition into the nonplanar conformation the energy gap  $\Delta E_V(T_1-S_0)$  for the sterically strained porphyrins decreases dramatically, being  $\sim 30.7$  kcal/mol (1.33 eV) for the planar conformation and  $\leq 10.4$  kcal/mol (0.45 eV) for nonplanar conformations. We are apt to believe that namely the decrease of the energy gap  $\Delta E_V(T_1-S_0)$  in this specific nonplanar conformation is the reason for the drastic reduction of the triplet state decays for OEP-*meso*Ph type molecules down to  $\tau_1^0 = 4.0 \mu s$  in degassed toluene solutions at 295 K.

As it is seen in Figure 5A, the transition of the OEP-*meso*Ph molecule from planar to nonplanar conformation in the excited triplet state is characterized by the energetic barrier of  $\sim 6.9$  kcal/mol. It is important to note that the nonplanar conformation



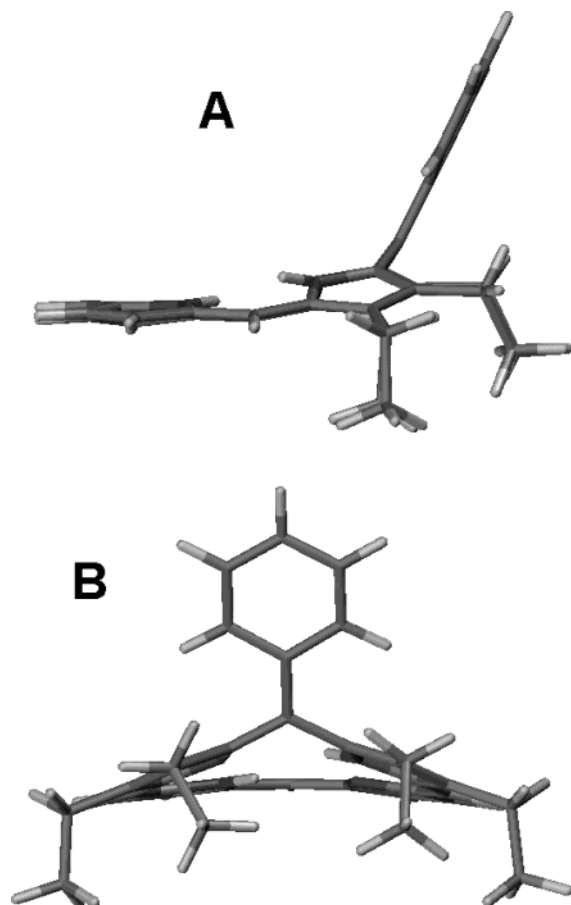


**Figure 4.** The nonplanar conformation of the OEP-*meso*Ph molecule in the  $T_1$  state depicted from two different sides. This conformation corresponds to the maximal overlap of the phenyl ring with  $\pi$ -conjugated porphyrin macrocycle (the dihedral angle  $\beta \sim 0^\circ$ ).

is by  $\sim 2.2$  kcal/mol more stable with respect to the planar one. Thus, considering the relatively small barrier height (6.9 kcal/mol), the OEP-*meso*Ph molecule may easily adopt the more energetically favorable nonplanar conformation. Since the transition into the nonplanar conformation is accompanied by the reduction of the energy gap  $\Delta E_V(T_1-S_0)$  by a factor of 3, this should lead to the considerable increase of the triplet state nonradiative rate constants that experimentally manifest in the drastic shortening of the triplet state lifetime for OEP-*meso*Ph ( $\tau_{T^0} = 4$   $\mu$ s) in comparison with  $\tau_{T^0} = 1.2$  ms for the OEP molecule.

For the triplet excited OEP-*meso*Ph(*o*-CH<sub>3</sub>) molecule with a bulky CH<sub>3</sub> group in the ortho position of the phenyl ring (Figure 5B), the energetic barrier of the transition to the nonplanar conformation increases up to 9.2 kcal/mol in comparison with 6.9 kcal/mol for OEP-*meso*Ph. At the same time, the energy of nonplanar conformation of OEP-*meso*Ph(*o*-CH<sub>3</sub>) turned out to be higher by the value of 4.8 kcal/mol than that calculated for the planar one. Consequently, an OEP-*meso*Ph(*o*-CH<sub>3</sub>) molecule in the triplet excited state would be preferentially in the planar conformation with large triplet-singlet energy gap  $\Delta E_V(T_1-S_0) = 1.33$  eV (30.7 kcal/mol) and, correspondingly, characterized by the small rate constant for the  $T_1$  state nonradiative deactivation  $T_1 \rightsquigarrow S_0$ . The last conclusion is in good agreement with the experimentally measured long triplet state lifetime  $\tau_{T^0} = 1.0$  ms for this molecule, which is only slightly shorter than that for the reference OEP molecule. It is of interest also that, according to calculations, for OEP-*meso*Ph(*o*-CH<sub>3</sub>) in the nonplanar conformation the value of the

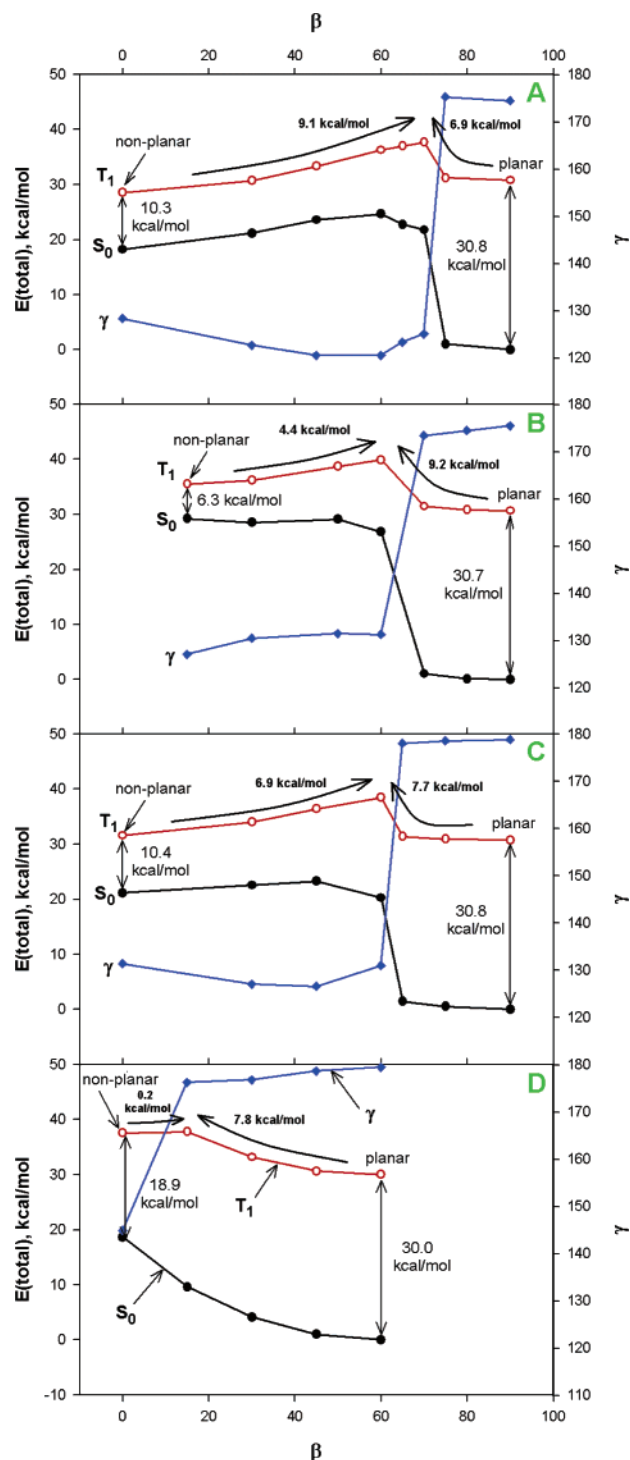


**Figure 5.** Theoretical dependence of the total energies,  $E(\text{total})$ , for the excited  $T_1$  (red curve, open circles) and ground  $S_0$  (black curve, filled circles) states as well as the angle  $\gamma$  value (blue curve, filled diamonds) on the dihedral angle  $\beta$ : OEP-*meso*Ph (A); OEP-*meso*Ph(*o*-CH<sub>3</sub>) (B); OMP-*meso*Ph (C); P-*meso*Ph (D). The lines connect the calculated points only for convenience. The energies of the ground  $S_0$ -state (black curves, filled circles) were calculated at the molecular geometry of the excited  $T_1$  state. It means that the vertical energy gap  $\Delta E_V(T_1-S_0)$  corresponds to the energy difference between the corresponding  $T_1$  and  $S_0$  curves for every compound. The total energy of the ground  $S_0$  state for planar conformations was taken to be  $E(S_0) = 0$  in all cases. The values of the  $\Delta E_V(T_1-S_0)$  energy gap for planar and nonplanar conformations, as well as the heights of the barriers of conformational transformations, are shown.

dihedral angle  $\beta$  is  $\sim 18^\circ$ , while for OEP-*meso*Ph and OMP-*meso*Ph molecules  $\beta \approx 0^\circ$ . Apparently, this difference is also

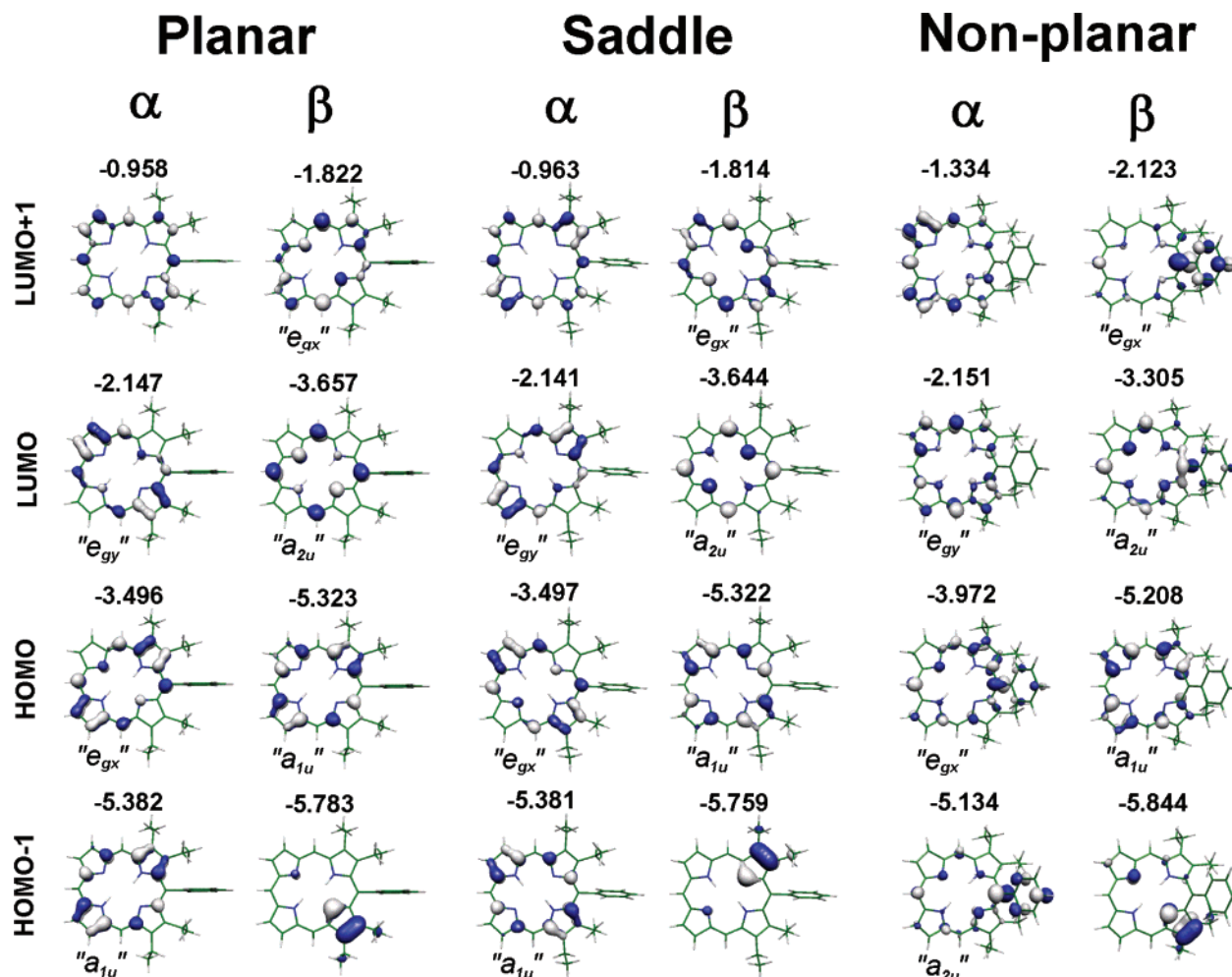


**Figure 6.** Frontier  $\alpha$  and  $\beta$  MOs of the planar, saddle-shaped, and nonplanar conformations for OEP-*meso*Ph molecule in the lowest triplet state. The energies of MOs (in eV) are indicated. The nodal properties of several MOs resemble the MOs of the metalloporphyrins of the  $D_{4h}$  point symmetry group, so they are marked according to the irreducible representations of the  $D_{4h}$  point symmetry group, taken in inverted commas.

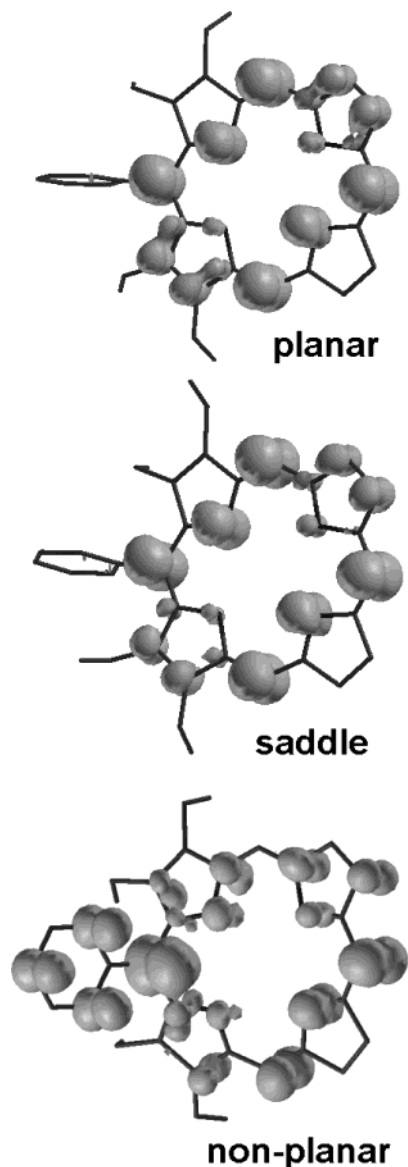
related to steric interactions of the bulky CH<sub>3</sub> group in the ortho position of the *meso*-phenyl with neighboring  $\beta$ -ethyl substituents and the porphyrin macrocycle.

Figure 5C shows that in the case of OMP-*meso*Ph molecule the calculated height of energy barrier for the conformational reorganization also increases slightly up to 7.7 kcal/mol in comparison with 6.9 kcal/mol for OEP-*meso*Ph. But in the case of OMP-*meso*Ph, the total energy in the T<sub>1</sub> state of the nonplanar conformation,  $E(\text{total})$  is by 0.8 kcal/mol higher than that of the planar conformation. Thus, the probability of the triplet excited OMP-*meso*Ph molecule to be in planar conformation should be greater than that in the nonplanar one. It means that, in the comparison with OEP-*meso*Ph (with favorable nonplanar conformation and  $\tau_T^0 = 4.0 \mu\text{s}$ ), the triplet state lifetime for the OMP-*meso*Ph molecule should be longer. In fact, our recent comparative experimental data for di-*meso*-phenyl-substituted octaalkylporphyrins<sup>27</sup> are in accord with this conclusion:  $\tau_T^0 = 16.5 \mu\text{s}$  for 5,15-PhOEP and  $\tau_T^0 = 177 \mu\text{s}$  for 5,15-PhOMP in degassed toluene at 295 K.

Finally, we considered mono-*meso*-phenyl-substituted porphyrine, P-*meso*Ph, without bulky  $\beta$ -alkyl substituents. As one may see in Figure 5D, for this compound the nonplanar conformation is characterized by just a very shallow minimum ( $\sim 0.2$  kcal/mol) on the triplet PES. At the same time, the triplet-singlet energy gap is large enough even for the nonplanar conformation:  $\Delta E_V(T_1-S_0) = 0.82$  eV (18.9 kcal/mol). This result points to the absence of an additional effective channel

for the triplet state deactivation due to the realization of nonplanar conformation with the decreased energy gap  $\Delta E_V(T_1-S_0)$  for P-*meso*Ph type molecules. Indeed, for tetramethyl-diethyl-mono-*meso*-phenyl porphyrin (not having bulky  $\beta$ -alkyl substituents neighboring the phenyl ring), the triplet state lifetime ( $\tau_T^0 = 1.64$  ms) is comparable to those found for planar OEP at the same conditions.<sup>22</sup>

**D. Electronic Properties of the Lowest Triplet State and Calculated T<sub>1</sub>  $\rightarrow$  T<sub>n</sub> Absorption Spectra.** Let us start with the consideration of electronic properties of the lowest triplet states for various conformations. For each conformation of OEP-*meso*Ph (planar, nonplanar, and saddle-shaped), 4  $\alpha$  and 4  $\beta$  HOMO and 3  $\alpha$  and 3  $\beta$  LUMO are depicted in Figure 6. As one may see on Figure 6, the nodal properties of MOs for planar and saddle-shaped conformations retain the main features of MOs for Me-porphyrins belonging to the  $D_{4h}$  point symmetry group. Therefore, we will describe MOs using notations for the  $D_{4h}$  group, taken in inverted commas. Thus, the nature of the T<sub>1</sub> state of planar and saddle-shape conformations may be described as "a<sub>2u</sub>"  $\otimes$  "e<sub>gx</sub>". As for the nonplanar conformation, the frontier MOs differ in form considerably from those obtained for planar and saddle-shape type conformations. One reason of that is the strong nonplanar distortion of the porphyrin macrocycle. Another reason seems to be the interaction of the MOs localized on the porphyrin with the MOs localized on the phenyl ring due to increased conjugation between porphyrin macrocycle and phenyl. It manifests itself in the strong admixture of the



**Figure 7.** Electron spin density distributions in the  $T_1$  state for the planar, saddle-shaped, and nonplanar conformations of OEP-*meso*Ph.

phenyl MO to  $\alpha$ -HOMO,  $\alpha$ -HOMO-1,  $\beta$ -LUMO and  $\beta$ -LUMO+1 in nonplanar conformation of OEP-*meso*Ph molecule. Spin density (SD) distributions (Figure 7) also show, that in nonplanar conformation the triplet wave function is delocalized over both porphyrin macrocycle and the phenyl ring, whereas it is localized almost completely on the porphyrin macrocycle in the cases of planar and saddle-shaped conformations. Thus, the direct comparison of MOs of the planar and saddle-shaped conformation, from one side, and the MOs of the nonplanar conformation, from the other side, is rather complicated. Still, the orbitals of “ $a_{1u}$ ”, “ $a_{2u}$ ”, and “ $e_g$ ” types may be distinguished by their characteristic nodal properties (see Figure 6). Thus, the  $T_1$  state of the nonplanar conformation is also formed by the excitation of the electron from the MO of “ $a_{2u}$ ” type to the “ $e_{gx}$ ” type MO.

The results calculated by the TD-DFT method of the  $T_1 \rightarrow T_n$  absorption spectra of OEP-*meso*Ph molecule in the nonplanar conformation are illustrated on Figure 2A (vertical rods, solid lines). One may see that the distinct feature of the calculated triplet–triplet absorption spectrum for the nonplanar conformation is the intense near-IR band that is significantly red-shifted with respect to the lowest absorption bands calculated for the

planar and saddle-shaped conformations (Figure 2B (dashed lines) and 2C). As was mentioned above, the experimental  $T_1 \rightarrow T_n$  absorption spectrum for the sterically hindered OEP-*meso*Ph molecule is characterized by the intense band with the maximum at 1000 nm, which is absent in  $T_1 \rightarrow T_n$  absorption spectra of OEP and OEP-*meso*Ph(*o*-CH<sub>3</sub>) molecules. The energies, oscillator strengths, and CI compositions of the allowed transitions of calculated  $T_1 \rightarrow T_n$  absorption spectra for OEP-*meso*Ph in the planar, saddle-shaped, and nonplanar conformations are collected in Table 1. One may see that the nature of the lowest allowed transition of the  $T_1 \rightarrow T_n$  spectrum for the nonplanar conformation is completely different from that of the planar and saddle-shaped conformations. For the nonplanar conformation, one-electron excitation of “ $e_{gx}$ ”  $\rightarrow$  “ $e_{gy}$ ” type is the major term contributing to the lowest allowed transition. The second large contribution is the one-electron excitation “ $a_{1u}$ ”  $\rightarrow$  “ $a_{2u}$ ”. At the same time the lowest allowed transition in the  $T_1 \rightarrow T_n$  spectrum of the planar conformation is dominated by the excitation of the electron from the MO, mostly localized on one of the pyrrole rings neighboring to the *meso*-phenyl, to the unoccupied MO of the  $a_{2u}$ -type.

Another distinguishing feature of the  $T_1 \rightarrow T_n$  spectrum of OEP-*meso*Ph molecule in the nonplanar conformation is the presence of the intensive band at 505 nm. Unfortunately, the experimental verification of this result seems to be rather difficult because of a strong overlap of  $T_1 \rightarrow T_n$  and  $S_0 \rightarrow S_n$  absorption spectra in this region. As one may see in Table 1, one-electron excitations from H-1  $\alpha$  and to L+1  $\beta$  provide the major contributions to this transition. Both H-1  $\alpha$  and L+1  $\beta$  are localized to a considerable extent on the phenyl ring.

Summarizing, from a remarkably good agreement of the experimental results and theoretical calculations on  $T_1 \rightarrow T_n$  absorption spectra in the red and near-IR region, it should be concluded that the triplet excited OEP-*meso*Ph molecule adopts the nonplanar conformation presented in Figure 4.

We also tried to separate the effect of macrocycle distortion from that of the increased conjugation between the porphyrin macrocycle and the *meso*-phenyl ring in the nonplanar conformation of OEP-*meso*Ph. With this purpose in mind,  $T_1 \rightarrow T_n$  absorption spectrum was calculated for the nonplanar conformation of the OEP-*meso*Ph molecule in which the phenyl ring was substituted by hydrogen, while the other geometrical parameters remained intact. The corresponding calculated transitions are indicated in Figure 2A with an asterisk. It follows from these data that the substitution of the phenyl ring by the hydrogen atom leads to the considerable (by  $\sim 2$  times) decrease in the intensity of the allowed transition in the region of 500 nm, which is slightly shifted to the blue in comparison with OEP molecule having the *meso*-phenyl ring. On the contrary, the energy and the oscillator strength of the longer wavelength transitions practically do not change. Thus, the appearance of the intense long-wavelength transition in the calculated  $T_1 \rightarrow T_n$  absorption spectrum for the nonplanar conformation of the OEP-*meso*Ph molecule is caused by the distortion of the porphyrin macrocycle. It is important to note that the vertical energy gap of the molecule without the phenyl ring remains small ( $\Delta E_V(T_1 \rightarrow S_0) = 0.51$  eV, compare with 0.45 eV for OEP-*meso*Ph). Therefore, the drastic reduction of vertical energy gap  $\Delta E_V(T_1 \rightarrow S_0)$  is also mostly due to the nonplanar distortion of the macrocycle.

#### IV. Summary and Conclusions

The detailed theoretical analysis of the nature of nonplanar conformations of sterically encumbered mono-*meso*-phenyl-substituted porphyrins, having different alkyl substituents in the



$\beta$ -positions, has been carried out for the excited triplet state. It was shown that triplet excited molecules of this type may adopt the highly nonplanar conformation characterized by the out-of-plane displacement of the single  $C_{m1}-C_1$  bond and the increased overlap of the porphyrin macrocycle and the *meso*-phenyl ring. Transition into this nonplanar conformation is accompanied by the essential decrease of the vertical energy gap  $\Delta E_V(T_1-S_0)$ , which is the reason for the drastic reduction of the triplet state decay time for the sterically strained porphyrins of this type. The calculated  $T_1 \rightarrow T_n$  transient absorption spectra for planar and nonplanar conformations of the investigated compounds have been compared with the corresponding experimental data obtained in our group earlier. An exceptionally good agreement of experimental results and theoretical calculations of  $T_1 \rightarrow T_n$  absorption spectra in the red and near-IR regions provides the additional support for the conformational reorganization leading to the formation of the highly nonplanar distortion of OEP-*meso*Ph molecule in the triplet excited state.

**Acknowledgment.** E.I.Z. and E.I.S. acknowledge support from the Belarus National Foundation for Basic Research (Grant Nr.Ph03-050).

**Supporting Information Available:** The  $T_1$  optimized geometries of all conformations for all compounds studied (in Cartesian coordinates). This material is available free of charge via the Internet at <http://pubs.acs.org>.

## References and Notes

- (1) McAuley, K. E.; Fyfe, P. K.; Cogdell, R. J.; Isaacs, N. W.; Jones, M. R. *FEBS Lett.* **2000**, *467*, 285.
- (2) Rhee, K.-H.; Morris, E. P.; Barber, J.; Kuhlbrandt, W. *Nature* **1998**, *396*, 283.
- (3) Deisenhofer, J.; Epp, O.; Miki, K.; Huber, R.; Michel, H. *J. Biol. Chem.* **1984**, *180*, 385.
- (4) Tronrud, D. E.; Schmid, M. F.; Matthews, B. W. *J. Mol. Biol.* **1986**, *188*, 443.
- (5) Shelnutt, J. A.; Song, X.-Z.; Ma, J.-G.; Jia, S.-L.; Jentzen, W.; Medforth, C. J. *Chem. Soc. Rev.* **1998**, *27*, 31.
- (6) Scheidt, W. R.; Lee, Y. J. In *Structure and Bonding*; Buchler, J. W., Ed.; Springer-Verlag: Berlin, 1987; Vol. 64, p 1.
- (7) Sessler, J. L.; Wang, B.; Springs, S. L.; Brown, C. T. In *Comprehensive Supramolecular Chemistry*; Marakami, Y., Ed.; Pergamon: New York, 1996; Vol. 4, p 311.
- (8) Chambron, J.-C.; Heitz, V.; Sauvage, J.-P. In *The Porphyrin Handbook*; Kadish, K. M.; Smith, K. M.; Guillard, R., Eds.; Academic Press: New York, 2000; Vol. 6, Ch. 40, p 1.
- (9) Zenkevich, E. I.; von Borczyskowski, C. In *Handbook of Polyelectrolytes and Their Applications*; Tripathy, S. K.; Kumar, J.; Nalwa, H. S., Eds.; American Scientific Publishers: Stevenson Ranch, CA, 2002; Vol. 2, Ch. 11, p 301–348.
- (10) Barkigia, K. M.; Berber, M. D.; Fajer, J.; Medforth, C. J.; Renner, M. W.; Smith, K. M. *J. Am. Chem. Soc.* **1990**, *112*, 8851.
- (11) Medforth, C. J.; Senge, M. O.; Smith, K. M.; Sparks, L. D.; Shelnutt, J. A. *J. Am. Chem. Soc.* **1992**, *114*, 9859.
- (12) Barkigia, K. M.; Renner, M. W.; Furenlid, L. R.; Medforth, C. J.; Smith, K. M.; Fajer, J. *J. Am. Chem. Soc.* **1993**, *115*, 3627.
- (13) Asano, M.; Kaizu, Y.; Kobayashi, H. *J. Chem. Phys.* **1988**, *89*, 6567.
- (14) Cunningham, K. L.; McNett, K. M.; Pierce, R. A.; Davis, K. A.; Harris, H. H.; Falck, D. M.; McMillin, D. R. *Inorg. Chem.* **1997**, *36*, 608.
- (15) Knyukshto, V. N.; Shulga, A. M.; Sagun, E. I.; Zenkevich, E. I. *Optics and Spectrosc. (Engl. Ed.)* **2002**, *92*, 53.
- (16) Renner, M. W.; Barkigia, K. M.; Zhang, U.; Medforth, C. J.; Fajer, J. *J. Am. Chem. Soc.* **1994**, *116*, 8582.
- (17) Senge, M. O.; Medforth, C. J.; Forsyth, T. P.; Lee, D. A.; Olmstead, H. M.; Jentzen, W.; Pandey, R. K.; Shelnutt, J. A.; Smith, K. M. *Inorg. Chem.* **1997**, *36*, 1149.
- (18) Kadish, K. M.; Van Caemelbecke, E.; D'Souza, F.; Lin, M.; Nurco, D. J.; Medforth, C. J.; Forsyth, T. P.; Kranttinger, B.; Smith, K. M.; Fukuzumi, S.; Nakanishi, I.; Shelnutt, J. A. *Inorg. Chem.* **1999**, *38*, 2188.
- (19) Takeda, J.; Ohya, T.; Sato, M. *Chem. Phys. Lett.* **1991**, *183*, 384.
- (20) Gentemann, S.; Nelson, N. Y.; Jaquinod, L.; Nurco, D. J.; Leung, S. H.; Medforth, C. J.; Smith, K. M.; Fajer, J.; Holten, D. *J. Phys. Chem. B* **1997**, *101*, 1247.
- (21) Sazanovich, I. V.; Galievsky, V. A.; van Hoek, A.; Schaafsma, T. J.; Malinovsky, V. L.; Holten, D.; Chirvony, V. S. *J. Phys. Chem. B* **2001**, *105*, 7818.
- (22) Knyukshto, V. N.; Zenkevich, E. I.; Sagun, E. I.; Shulga, A. M.; Bachilo, S. M. *Chem. Phys. Lett.* **1998**, *297*, 97.
- (23) Knyukshto, V. N.; Sagun, E. I.; Shulga, A. M.; Bachilo, S. M.; Zenkevich, E. I. *Chem. Phys. Rep.* **1999**, *18*, 855.
- (24) Knyukshto, V.; Zenkevich, E.; Sagun, E.; Shulga, A.; Bachilo, S. *J. Fluoresc.* **2000**, *10*, 55.
- (25) Andreasson, J.; Zetterqvist, H.; Kajanous, J.; Martensson, J.; Albinsson, B. *J. Phys. Chem. A* **2000**, *104*, 9307.
- (26) Kyrychenko, A.; Andreasson, J.; Martensson, J.; Albinsson, B. *J. Phys. Chem. B* **2002**, *106*, 12613.
- (27) Zenkevich, E. I.; Sagun, E. I.; Knyukshto, V. N.; Shulga, A. M.; Grubina, L. A.; Golubchikov, O. A.; Semeikin, A. S. In *Materials of the IX International Conference "Chemistry of Porphyrins and their Analogs"*; Ageeva, T. A., Ed.; Ivanovo State University of Chemistry and Technology: Ivanovo, Russia, 2003; p 194–196.
- (28) Michaeli, S.; Soffer, S.; Levanon, H.; Senge, M.; Kalish, W. J. *Phys. Chem. A* **1999**, *103*, 1950.
- (29) Knyukshto, V. N.; Sagun, E. I.; Shulga, A. M.; Bachilo, S. M.; Starukhin, D. A.; Zenkevich, E. I. *Optics Spectrosc. (Engl. Ed.)* **2001**, *90*, 67.
- (30) Stewart, J. J. P. *J. Comput. Chem.* **1989**, *10*, 209.
- (31) Stewart, J. J. P. *J. Comput. Chem.* **1989**, *10*, 221.
- (32) Pople, J. A.; Nesbet, R. K. *J. Chem. Phys.* **1954**, *22*, 571.
- (33) Becke, A. D. *J. Chem. Phys.* **1993**, *98*, 5648.
- (34) Lee, C.; Yang, W.; Parr, R. G. *Phys. Rev. B* **1988**, *37*, 785.
- (35) Roothan, C. C. J. *Rev. Mod. Phys.* **1951**, *23*, 69.
- (36) Bauernschmitt, R.; Ahlrichs, R. *Chem. Phys. Lett.* **1996**, *256*, 454.
- (37) Casida, M. E.; Jamorski, C.; Casida, K. C.; Salahub, D. R. *J. Chem. Phys.* **1998**, *108*, 4439.
- (38) Ditchfield, R.; Hehre, W. J.; Pople, J. A. *J. Chem. Phys.* **1971**, *54*, 724.
- (39) Hehre, W. J.; Ditchfield, R.; Pople, J. A. *J. Chem. Phys.* **1972**, *56*, 2257.
- (40) Frisch, M. J.; Trucks, G. W.; Schlegel, H. B.; Scuseria, G. E.; Robb, M. A.; Cheeseman, J. R.; Zakrzewski, V. G.; Montgomery, J. A., Jr.; Stratmann, R. E.; Burant, J. C.; Dapprich, S.; Millam, J. M.; Daniels, A. D.; Kudin, K. N.; Strain, M. C.; Farkas, O.; Tomasi, J.; Barone, V.; Cossi, M.; Cammi, R.; Mennucci, B.; Pomelli, C.; Adamo, C.; Clifford, S.; Ochterski, J.; Petersson, G. A.; Ayala, P. Y.; Cui, Q.; Morokuma, K.; Malick, D. K.; Rabuck, A. D.; Raghavachari, K.; Foresman, J. B.; Cioslowski, J.; Ortiz, J. V.; Stefanov, B. B.; Liu, G.; Liashenko, A.; Piskorz, P.; Komaromi, I.; Gomperts, R.; Martin, R. L.; Fox, D. J.; Keith, T.; Al-Laham, M. A.; Peng, C. Y.; Nanayakkara, A.; Gonzalez, C.; Challacombe, M.; Gill, P. M. W.; Johnson, B. G.; Chen, W.; Wong, M. W.; Andres, J. L.; Head-Gordon, M.; Replogle, E. S.; Pople, J. A. *Gaussian 98*, revision A.11; Gaussian, Inc.: Pittsburgh, PA, 1998.